# Poly(vinyl chloride)/$CaCO_3$ Nanocomposites: Influence of Surface Treatments on the Properties

**Irene Bonadies,[1] Maurizio Avella,[2] Roberto Avolio,[1] Cosimo Carfagna,[2] Maria Emanuela Errico,[2] Gennaro Gentile[2]**

[1]*University of Naples "Federico II," Department of Engineering Materials and Production, P. le Tecchio, 80-80125 Napoli, Italy*
[2]*Institute of Polymer Chemistry and Technology, National Research Council, Via Campi Flegrei, 34-80078 Pozzuoli (Na), Italy*

Received 28 April 2011; accepted 28 April 2011
DOI 10.1002/app.34770
Published online 10 August 2011 in Wiley Online Library (wileyonlinelibrary.com).

**ABSTRACT:** Poly(vinyl chloride) (PVC)-based nanocomposites containing calcium carbonate nanoparticles ($CaCO_3$) were prepared. Different nanoparticle surface modifiers were selected and tested to promote matrix/filler interactions and, consequently, to obtain high-performance materials. In particular, the nanoparticles were modified with poly(acrylic acid) (PAA) and poly (butadiene-*co*-acrylonitrile-*co*-acrylic acid) (PBAA). For comparison, PVC-based materials, with the addition of commercial neat and stearic acid modified $CaCO_3$, were also prepared. The influence of $CaCO_3$ and surface modifiers on the gelation, thermal properties, thermal stability, and mechanical properties of PVC was studied. The gelation time of the rigid PVC/$CaCO_3$ composites decreased as a function of the percentage and surface treatment of $CaCO_3$. Morphological analysis proved the effectiveness of PAA and PBAA as surface modifiers; they obtained for the corresponding materials a typical nanostructured morphology. A significant improvement in the PVC thermal stability was recorded with the addition of neat and stearic acid modified $CaCO_3$. Finally, mechanical tests showed an increase in the flexural strength and toughness of PVC as a function of the nanoparticle surface modifier. © 2011 Wiley Periodicals, Inc. J Appl Polym Sci 122: 3590–3598, 2011

**Key words:** interfaces; mechanical properties; morphology; nanocomposites; structure–property relations

## INTRODUCTION

Poly(vinyl chloride) (PVC) is the second most used plastic material worldwide. Its good mechanical and electrical properties, good resistance to corrosion and weathering, good processability, and wide range of properties obtained by compounding with plasticizer, fillers, lubricants, impact modifier, processing aids, pigments, and stabilizer make PVC one of the most versatile thermoplastics.[1] However, its low thermal stability and brittleness can be a limit in certain applications. Although elastomers have been widely used to toughen rigid PVC, their incorporation not only leads to decreased strength, heat stability, and modulus but also increases the cost of such composites.[2–7]

Therefore, to broaden the range of applications of PVC, it is necessary to develop new, low-cost, effective toughening strategies.

Nowadays, the development of nanocomposites is an effective answer to continuous efforts to realize high performance, good processability, and low cost materials.[8–13] As it is known, the extraordinary changes of properties in nanocomposites mainly depend on the so called nanoeffect.[14]

When a filler is added to the polymer matrix, an interphase of finite width, whose properties differ from the neighboring phases, is formed as a result of strong filler/polymer interactions. The interphase can be 2–50 nm thick, and due to the enormous surface area of the nanofillers, in nanocomposites, it can represent up to 50 vol % of the whole material. The polymeric material close to the interface gains additional properties different from those of the filler and polymer and gives rise to the new characteristics of the nanocomposite.[15–18] In this respect, the greatest challenge in the development of high-performance nanocomposites is related to the achievement of tailored interphase properties through the maximization of polymer–nanoparticle interactions.

Extensive research work has been carried out to correlate, as an example, the nanoparticle reinforcing ability with the strength of interfacial adhesion.[19–22]

To this aim, many studies have been focused on surface nanoparticle treatments, which consist of the grafting of organic molecules and/or the addition of interfacial agents to better control the nanofiller dispersion and to promote strong interactions between phases.

Among different nanosized fillers, such as montmorillonite, silica, and aluminum oxide,[23–29]

*Correspondence to:* M. E. Errico (mariaemanuela.errico@ictp.cnr.it).

nanocalcium carbonate ($CaCO_3$) is one of the most commonly used in the preparation of PVC nanocomposites because of its low cost.[30–33]

There have been several studies demonstrating the influence of calcium carbonate, with or without an additional coating agent, on the properties of PVC. These researches have demonstrated that the highest performances can be achieved if the interfacial adhesion between the filler and polymer matrix is optimized. Other studies have focused on ternary nanocomposites, in which an additional rubber phase was included as an interfacial modifier to realize PVC/$CaCO_3$ nanocomposites characterized by an improved impact strength.[34–38]

In this article, results regarding the preparation and characterization of rigid PVC-based materials containing differently modified calcium carbonate nanoparticles ($CaCO_3$) are discussed. In particular, poly(acrylic acid) (PAA) and poly(butadiene-*co*-acrylonitrile-*co*-acrylic) acid (PBAA) were selected as $CaCO_3$ surface modifiers. This selection was based on both the well-known compatibility of these polymers with PVC and their elastic properties.[39] In this respect, the purpose was not only to obtain a good dispersion level of nanophase but also to improve interactions between the components, as well as to modulate the properties of the interphase and, then, of the whole material. Nanocomposites containing neat and commercial stearic acid modified $CaCO_3$ were also prepared for comparison.

The influence of the filler surface treatment on the microstructure, morphology, thermal stability, and mechanical properties was investigated.

## EXPERIMENTAL

### Materials

PVC with a *K* value (Fikentscher-k value) viscosity index of 67 was kindly supplied by Solvin S. A. (Brussels, Belgium).

Nano-$CaCO_3$ (calcite, 40-nm mean size with a narrow size distribution, Brunauer–Emmett–Teller surface area = 40 $m^2/g$, approximate density = 2.7 $g/cm^3$), either neat or modified with 3 wt % stearic acid, was supplied by Nachmann S. R. L. (Milano, Italy).

An organic-based one-pack stabilizing/lubricant system (Reapak G-TU 1130 XO) was supplied by Reagens S. P. A. (Bologna, Italy).

PAA (medium viscous, Fluka; a Sigma-Aldrich company, St. Louis, MO ) and PBAA (0.06 carboxyl equiv/100 g, Polysciences, Inc., Warrington, PA) were used without further purification.

### $CaCO_3$ surface treatments

The surface modification of $CaCO_3$ with PAA or PBAA was carried out in solution. In particular, on the basis of the PAA and PBAA solubility, either ethanol or chloroform was selected as the solvent. $CaCO_3$ (7 g) was dispersed in 50 mL of ethanol and in 50 mL of chloroform with an ultrasonic homogenizer (MSE equipment Measuring and Scientific Equipment, London, UK) for 5 min with a progressive increase in the power amplitude from 6 to 12-μm peak to peak. Then, to these dispersions, 50 mL of PAA–ethanol solution (0.08 g/mL) or 50 mL of PBAA–chloroform solution (0.08 g/mL) were added, respectively. The reaction proceeded at 80°C for 2 h under mechanical stirring. The modified particles were recovered by centrifugation and repeatedly washed with ethanol or chloroform to remove unreacted PAA or PBAA and then dried in a vacuum oven at 100°C overnight.

### Preparation of the PVC/$CaCO_3$ nanocomposites

The preparation of the PVC-based nanocomposites was performed in two steps. In the first one, 3 wt % with respect to PVC powder of a stabilizing/lubricant mixture and a certain amount of nano-$CaCO_3$ (1 and 3 wt % with respect to PVC plus the stabilizing/lubricant mixture) were added to PVC powder. This compound was mixed in a high-speed mixer for 10 min to prepare a dry blend. In the second step, the dry blend was processed in a Plastograph internal mixer (Brabender GmbH & Co. KG, Duisburg, Germany) at 170°C for 10 min and at a 64-rpm mixing speed.

Successively, the obtained material was pelletized and then compression-molded in a heated press at 190°C 0 bar for 3 min; then the pressure was raised and kept at 200 bar for 2 min. The press plates, equipped with cooling coils, were quickly cooled to room temperature by cold water, and then, the pressure was released. Sheets (thickness = 3.5 mm) were obtained and used for all characterizations.

### Techniques

Solid-state $^{13}$C-NMR cross-polarization/magic angle spinning (CP–MAS) spectra were collected at 100.47 MHz on a Bruker Avance II 400 spectrometer (Bruker Inc. Billerica, MA) operating at a static field of 9.4 T and equipped with a 4-mm MAS probe. PAA–$CaCO_3$ and PBAA–$CaCO_3$ were packed into 4-mm zirconium rotors sealed with Kel-F caps. Solid-state $^{13}$C-NMR CP–MAS spectra were carried out with a relaxation delay of 2 s and a contact time of 1.5 ms. The $^1$H $\pi/2$ pulse width was 2.80 μs, and the cross-polarization was performed with the application of a variable spin-lock sequence RAMP–CP–MAS.[40,41] Spectra were obtained at a spinning speed of 6.5 kHz with 1024 data points in the time domain, zero-filled, and Fourier transformed. Ten thousand scans were collected for each sample.

Thermogravimetric analyses (TGAs) were carried out with a PerkinElmer thermogravimetric analyzer (Pyris Diamond; PerkinElmer Inc. Waltham, MA). Measurements were performed in the range 30–800°C at a heating rate of 10°C/min in $N_2$ flux (100 mL/min). The weight loss versus temperature traces were recorded, and the temperature corresponding to the 1% weight loss (Tonset) was taken as the starting point of the degradation process.

Differential scanning calorimetry (DSC) analyses were carried out with a Mettler-Toledo (Columbus, OH) DSC 822 in $N_2$ flux with the following temperature program: heating from 25 to 225°C, cooling from 225 to 0°C, and heating from 0 to 235°C. The heating/cooling rate was set to 10°C/min, and the values of enthalpy were calculated from the second heating run. The crystallinity content was calculated with consideration of the effective polymer content and with the enthalpy of fusion of PVC in the fully crystalline state of 167 J/g.[42]

Morphological analysis of the composites was performed with scanning electron microscopy (SEM; Philips XL20 series; Philips N.V. Amsterdam, The Netherlands) on the fractured surface of the samples after impact testing. Before observation, samples were coated with an Au–Pd alloy with an SEM coating device (SEM BALTEC MED 020; Bal-Tec A.G. Balzers, Liechtenstein).

Fracture tests were carried out with a Charpy Ceast Resil impactor equipped with a DAS 4000 acquisition system with an impact energy of 3.6 J and an impact speed of 1 m/s. Samples (10.0 mm wide, 3.5 mm thick, and 60 mm long) with a notch depth-to-width ratio of 0.3 and a span length of 48 mm were fractured at room temperature according to ASTM D 256.[43]

Three-point flexural testing was performed on an Instron (an Illinois Tool Works Inc. Company, Glenview, IL) 4504 testing machine at a test speed of 1 mm/min to evaluate both the flexural strength and flexural modulus according to ASTM D 790.[44]

## RESULTS AND DISCUSSION

As it is known, interactions occurring between nanosized fillers and the bulk polymer matrix lead to the formation of an interphase, which markedly affects the properties of materials.[45] In this respect, the chemical surface treatment of fillers can be an effective strategy to make more hydrophobic the nanoparticle surface and thus prevent filler agglomeration phenomena and, at the same time, to promote interactions.[46] To this aim, two different coating agents were selected; in particular, the $CaCO_3$ surface was modified with PAA and with PBAA. Their selection depended on the possibility of improving the PVC/nanoparticle compatibility because of the compatibility of PVC with the acrylic surface modifiers[39] and to modulate the properties of the interphase and then of the whole material. The surface treatment was achieved in solution and was based on ionic interactions occurring between the surface $Ca^{2+}$ ions and the carboxyl groups of PAA or PBAA.

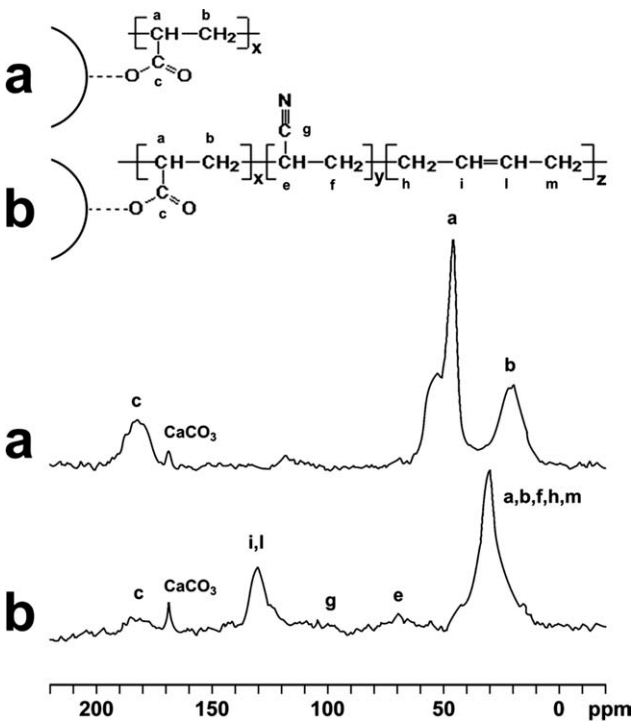


**Figure 1** $^{13}C$ CP–MAS spectra of (a) PAA–$CaCO_3$ and (b) PBAA–$CaCO_3$.

The grafting was verified by means of solid-state NMR. $^{13}C$ cross-polarization experiments (CP–MAS) were performed on both modified nanophases (PAA–$CaCO_3$ and PBAA–$CaCO_3$). In Figure 1, the spectra of PAA–$CaCO_3$ [Fig. 1(a)] and PBAA–$CaCO_3$ [Fig. 1(b)] with the corresponding assignment of signals are illustrated. These spectra showed resonances clearly attributable to the organic functionalities of PAA and PBAA in addition to the resonance of $CaCO_3$ carbonate group at 168.5 ppm.

It is well known that experiments in $^{13}C$–$^{1}H$ cross-polarization mainly reveal signals of carbon atoms that are directly linked to hydrogens and/or dipolar coupled to them. As a matter of fact, the appearance of carbonate group signal was due to the transfer of proton magnetization from the coupling agent (PAA or PBAA) to the $CaCO_3$ surface. In this respect, the close proximity of the organic modifier to the nanoparticle surface was demonstrated.

The theoretical structure of the $CaCO_3$ modified with PAA or PBAA is sketched in Scheme 1.

The amount of acrylic modifiers on the surface was evaluated by TGA as the weight loss percentage in the temperature range in which neat calcium carbonate did not show any thermal degradation. It was estimated to be 2 wt % for both PAA and PBAA.

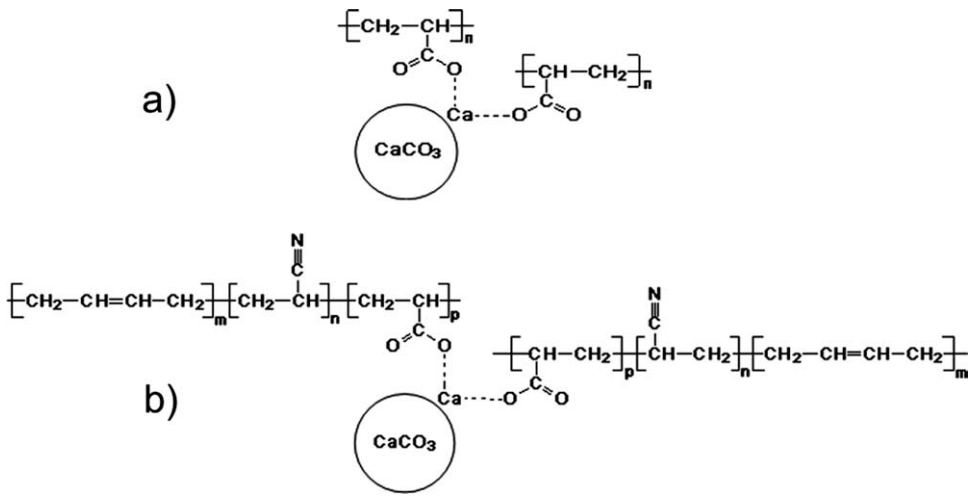


**Scheme 1** Schematic structure: (a) PAA–$CaCO_3$ and (b) PBAA–$CaCO_3$.

The modified nanoparticles were employed for the preparation of PVC-based nanocomposites according to the procedure described in a previous section. Composites containing neat and commercial stearic acid modified $CaCO_3$ were also prepared for comparison. Table I reviews the prepared materials.

### Gelation process and thermal analysis

The properties of the PVC-based materials were strongly dependent on the structure of the starting PVC resin and on the processing conditions.

As known, PVC presents a very complex hierarchical particle structure in which grains (~200 μm) consist of the agglomeration of 1–2 μm sized primary particles. These primary particles are formed by polymer chains tied together by a small amount (5–10%) of crystalline phase (primary crystals).[47]

During processing, under shear and heat, the grains are crushed, and the interface between the primary particles progressively disappears. This allows the formation of molecular entanglements by diffusion, whereas the crystals start melting. This process, denoted as *gelation,* is the first stage of any transformation process of PVC, leads to the transformation of an incoherent powder in a processable melt, and has a big influence on the mechanical properties of the material.

It is only at this stage that homogenization and mixing of the additives takes place and makes the gelation time an important process parameter.

After processing, during the cooling down, new ordered entities, denominated secondary crystallites, are formed,[48–50] and residual primary crystals can partly recrystallize. As a result, in processed PVC, the initial particulate structure is transformed in a three-dimensional macromolecular network. The amount of residual primary and produced secondary crystallites depends on the processing conditions and strongly influences the physical and mechanical properties of the PVC-based materials.[51–53]

The gelation process of neat PVC and the PVC-based composites as a function of the nanoparticle content and surface modifier was monitored by analysis of the torque curve recorded during melt mixing.

As an example, a typical PVC torque curve is reported in Figure 2.

**TABLE I**
**Materials and Corresponding Codes**

| Code | $CaCO_3$ (wt %) | Surface modifier | Modifier (vs $CaCO_3$; wt %) |
|---|---|---|---|
| PVC | — | — | — |
| A1 | 1 | — | — |
| A3 | 3 | — | — |
| B1 | 1 | Stearic acid | 3 |
| B3 | 3 | Stearic acid | 3 |
| C1 | 1 | PAA | 2 |
| C3 | 3 | PAA | 2 |
| D1 | 1 | PBAA | 2 |
| D3 | 3 | PBAA | 2 |

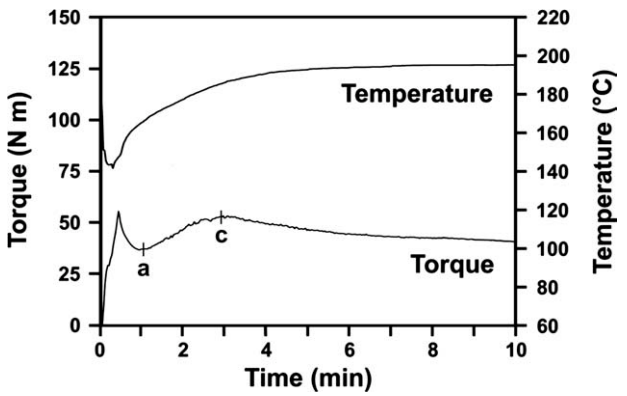


**Figure 2** PVC torque curve recorded during melt processing.

**TABLE II**
**Gelation Time Values as a Function of $CaCO_3$ Content and Surface Treatment**

| Sample | Gelation time (min) |
|---|---|
| PVC | 1.87 |
| A1 | 1.28 |
| A3 | 0.93 |
| B1 | 1.11 |
| B3 | 0.78 |
| C1 | 1.61 |
| C3 | 1.39 |
| D1 | 1.69 |
| D3 | 1.53 |

After the loading stage, a significant increase in the torque was registered; it corresponded to the initial grain compression and densification, with a simultaneous decrease of the temperature measured in the chamber. As a result of shearing, grains gradually disintegrated, whereas the particles, which were in contact with the chamber wall, started flowing. Then, the molten fraction increased the flowability of the remaining polymer grains (lubrication effect) and determined the minimum point a of the torque value. After that, material gelation started with a corresponding increase in torque, until point c. The maximum point could be ascribed to the formation of a macromolecular network, which resulted from the breakdown of the original resin particle and chain interdiffusion.[52] At this point, the homogenization and dispersion of the fillers and additives started, the temperature increased, and the torque decreased, with both approaching a plateau.[54]

The time elapsed between the points a and c of the torque curve was defined as the *gelation time*.[55]

All of the PVC/$CaCO_3$ torque curves showed a similar gelation behavior, but the gelation time depended on the filler content and surface modifier.

In particular, as shown in Table II, the gelation time decreased sharply for systems A and B and, to a lesser extent, for both acrylic modified particles. With 3 wt % particles, the decrease is always stronger than with 1 wt %.

The effect of processing on the compound microstructure was also investigated by means of DSC, by measurement of the residual content of primary crystals and the newly formed secondary ones.

As reported in Figure 3, two endothermic peaks, very broad because of the presence of defects and a large size distribution, were distinguishable in the thermograms and attributable to the melting of secondary crystallites (lowest temperatures range) and primary crystallites (highest temperature range), respectively.[56] From these data, the degree of gelation ($G$) could be calculated, as follows:

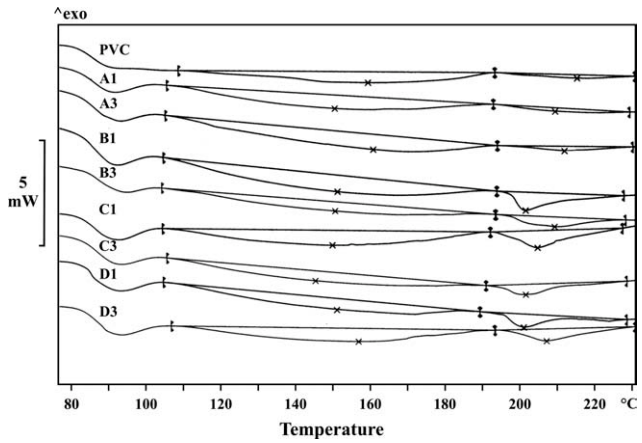


**Figure 3** DSC traces of PVC and PVC-based nanocomposites.

$$G = \frac{HA}{HA + HB} \times 100$$

where $H_A$ and $H_B$ are the heats of fusion of the secondary and primary crystallites, respectively.[57]

It could be noticed that for systems containing modified $CaCO_3$ nanoparticles (B, C, and D), $G$ was lower, with more than twice the residual primary crystallites with respect to the neat PVC and system A (see Table III). The influence of the fillers on the gelation behavior was, thus, dependent on the surface treatment.

On the basis of the smaller dimension of $CaCO_3$ ($\sim$ 40 nm) with respect to PVC grains ($\sim$ 200 μm) and primary particles ($\sim$ 2 μm), the rigid, noninteracting nanofiller particles (system A) could be thought of as acting like a grinding or abrading medium, accelerating the crushing of the particles and promoting a faster mixing and a more effective frictional heating.

The stearic acid coated particles, while lowering the gelation time, led to a lower $G$. Thus, their effect could be ascribed to a lubrication/plasticization of the PVC particle boundaries.

**TABLE III**
**DSC Results of the PVC and PVC-Based Materials**

| Sample | Secondary crystallites (%) | Primary crystallites (%) | $G$ |
|---|---|---|---|
| PVC | 4.2 | 0.5 | 89.4 |
| A1 | 5.2 | 0.4 | 92.9 |
| A3 | 3.9 | 0.4 | 90.7 |
| B1 | 5.9 | 1.4 | 80.8 |
| B3 | 3.4 | 1.1 | 75.6 |
| C1 | 5.2 | 1.8 | 74.3 |
| C3 | 3.6 | 1.1 | 76.6 |
| D1 | 4.4 | 1.3 | 77.2 |
| D3 | 3.8 | 1.2 | 76.0 |

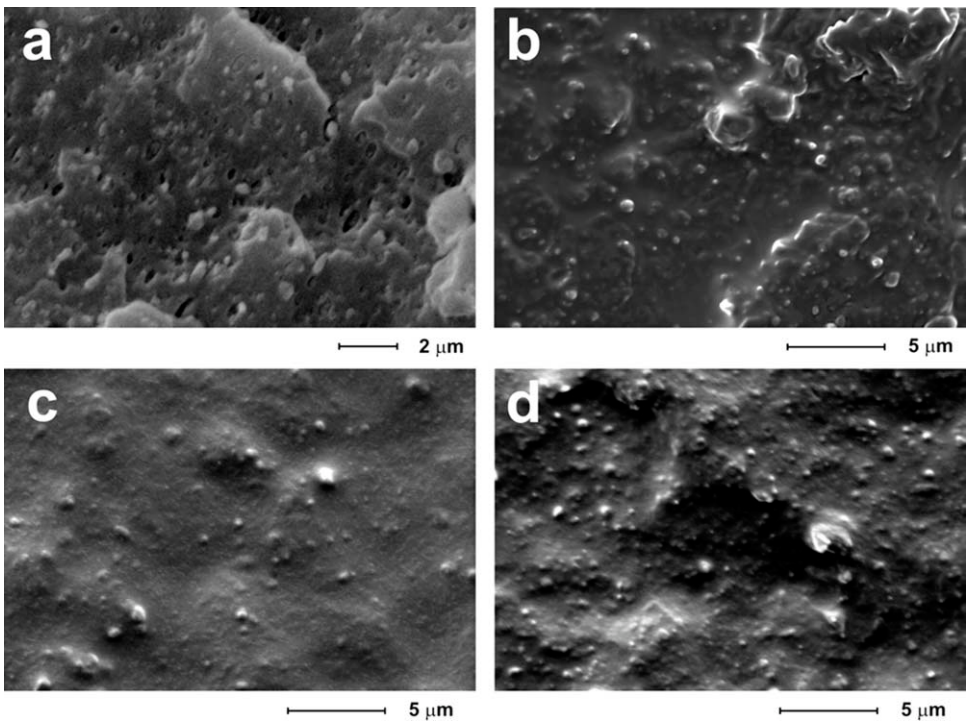


**Figure 4** SEM micrograph of the fractured surface of samples (a) A3, (b) B3, (c) C3, and (d) D3.

Finally, the PAA- and PBAA-treated particles further lowered the gelation level with a minor effect on the gelation time.

The gelation level, as an index of the residual primary crystallinity, could have a big influence on the mechanical properties of PVC and PVC-based materials.[58]

## Morphological analysis

In Figure 4, SEM micrographs of the fractured surface of materials A–D, containing the highest amount of $CaCO_3$ [3 wt %; Fig. 4(a–d)], are reported as examples.

Morphological characterization proved the effectiveness of PAA and PBAA as coupling agents, which promoted the typical nanocomposite structure; the nanoparticles appeared finely and homogeneously dispersed in the matrix. Moreover, the absence of voids along the particle surface suggested strong interfacial adhesion between the polymer and nanophase [Fig. 4(c,d)]. On the contrary, in materials containing neat $CaCO_3$, serious debonding and agglomeration phenomena occurred [Fig. 4(a)]. In fact, nanoparticles mainly pulled out, leaving voids on the surface and, thus, demonstrating the absence of bonding and compatibility between the polymer and $CaCO_3$.

Finally, the presence of the sole stearic acid, although preventing the nanoparticle pullout, at the same time, was not able to prevent the agglomeration phenomena [Fig. 4(b)]. In this respect, stearic acid could not be considered a proper coupling agent.

These findings could be explained on the basis of interactions established between components. In system A, nanoparticle/nanoparticle interactions resulted dominantly as a consequence of a very high filler surface energy and the chemical incompatibility between the polymer and nanosized phase. In the case of systems B, the presence of an organic layer (stearic acid) on the surface permitted to lower the surface energy, but at the same time, it did not result in compatibility with PVC. In this respect, strong particle/surface modifier and weak surface modifier/polymer matrix interactions could be hypothesized.

Finally, in the case of systems C and D, both the surface modifier/filler and surface modifier/polymer interactions were strong enough to achieve a nanometric dispersion and a good $CaCO_3$/PVC interfacial adhesion. In this respect, PAA and PBAA could be defined as coupling agents.

## TGA

The thermal degradation of PVC occurs in two steps[59] in a very wide temperature range (200÷600°C), involving different sequential and competitive processes, such as dehydrochlorination, auto-oxidation, chemical chain scission, and cross-linking. The early stage, up to 400°C, consists of the loss of hydrogen chloride (HCl) molecules. This is an autocatalytic reaction, and once started, the

**TABLE IV**
**TGA Results of the PVC and PVC-Based Materials**

| Sample | $T_{onset}$ (°C) |
|---|---|
| PVC | 244 |
| A1 | 252 |
| A3 | 260 |
| B1 | 250 |
| B3 | 256 |
| C1 | 240 |
| C3 | 253 |
| D1 | 243 |
| D3 | 247 |

evolved HCl catalyze the elimination of further acid molecules. The elimination of HCl leads to the formation of polyene sequences on the polymer backbone, which cause discoloration and changes in the physical properties. At higher temperatures, the polyenes undergo secondary competitive reactions, such as intramolecular cyclization and intermolecular crosslinking. Finally, the decomposition of the crosslinked intermediates leads to the formation of a carbon residue (char) and aromatic compounds.

As reported in Table IV, the addition of neat and stearic acid modified $CaCO_3$ increased the onset temperature of the PVC degradation ($T_{onset}$) process up to 16°C, whereas the temperature corresponding to the maximum decomposition rate was not affected by the presence of the filler. In Figure 5, as an example, the starting stage of the degradation process of PVC as compared to that of system A is illustrated.

In the case of materials containing acrylic acid modified nanoparticles, systems C and D, the PVC thermal stability was almost unchanged.

These results could be explained by the fact that calcium ions on the nanoparticle surface were able to scavenge part of produced HCl and, thus, slow down the autocatalytic dehydrochlorination process.[60] In the case of modified nanoparticles, although surface calcium ions should have been partially unavailable as a consequence of the surface treatment, the thermal stability of the surface modifier had to be taken into account. The degradation of the stearic acid started at temperatures lower than PVC,[61] so the nanoparticle surface was uncoated, and the calcium ions became available to react with hydrochloric acid. On the contrary, the degradation of PAA and PBAA occurred in the same range (PBAA) or at higher temperatures (PAA) compared to that of PVC.[62,63] The surface calcium ions were, thus, not available, and then, no influence on the degradation stability in the corresponding materials was obtained.

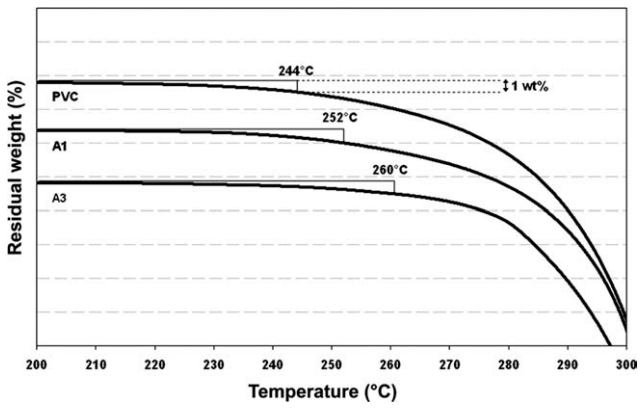


**Figure 5** TGA traces showing the onset of the degradation process for PVC and the A1 and A3 systems.

## Mechanical properties

Mechanical analysis of neat PVC and PVC-based nanocomposites was performed at low (flexural) and high (impact) deformation rates. The flexural modulus, flexural strength, and stress intensity factor ($K_C$) values of the PVC-based nanocomposites are reported in Table V.

As reported, the flexural properties of PVC were not influenced by the addition of neat (system A) and stearic acid coated nanoparticles (systems B). On the contrary, in system C (PAA-coated $CaCO_3$) and system D (PBAA-coated $CaCO_3$), slight increases of up to 10% in the flexural modulus and up to 20% in the flexural strength were recorded, independent of the filler content.

The modulus in composites is usually insensitive to the interfacial adhesion, being measured at very small deformations when physical contact of the components is sufficient to transfer the stress. The small differences recorded between the acrylic-functionalized and the other systems can be merely ascribed to the better dispersion achieved with the former coatings. Big aggregates have, in fact, bad mechanical properties and give no contribution to load bearing.

On the contrary, the mechanical parameters at break, such as flexural strength, are strongly dependent on the interfacial adhesion between components, being the interface responsible for transferring the stress from the matrix to the nanoparticle

**TABLE V**
**Mechanical Parameters of the PVC and PVC-Based Materials**

| Sample | Flexural modulus (MPa) | Flexural strength (MPa) | $K_C$ (MPa $m^{1/2}$) |
|---|---|---|---|
| PVC | 2309 ± 216 | 76 ± 4 | 2.30 ± 0.05 |
| A1 | 2296 ± 124 | 74 ± 3 | 2.49 ± 0.14 |
| A3 | 2343 ± 148 | 78 ± 3 | 2.55 ± 0.18 |
| B1 | 2268 ± 150 | 81 ± 3 | 2.66 ± 0.13 |
| B3 | 2321 ± 108 | 73 ± 3 | 2.78 ± 0.23 |
| C1 | 2600 ± 79 | 90 ± 3 | 2.96 ± 0.15 |
| C3 | 2692 ± 48 | 92 ± 2 | 2.82 ± 0.05 |
| D1 | 2518 ± 83 | 91 ± 3 | 2.88 ± 0.07 |
| D3 | 2517 ± 53 | 90 ± 3 | 3.02 ± 0.10 |

phase.[64] The failure of the interface would vanish any reinforcing effect of the filler and even lead to a premature failure of the whole material. Thus, the increase in the flexural strength for the acrylic-coated systems was proof of the effectiveness of PAA and PBAA as coupling agents in the promotion of a strong PVC/nanofiller interaction, as suggested by morphological analysis.

The impact toughness of the PVC and PVC-based materials was analyzed by calculation of the critical $K_C$. This parameter defines the stress field at fracture and describes the crack initiation conditions for fractures that are completely elastic according to a linear elastic fracture mechanics (LEFM).

As reported in Table V, an increase in the $K_C$ parameter was recorded for system B ($\leq$20%) and for systems C and D ($\leq$30%). Interestingly, for these systems, a lower $G$, that is, a bigger amount of residual primary crystallites, was found by DSC analysis (see Table III). The impact toughness of PVC measured versus gelation level usually shows a maximum corresponding to an optimum value of this parameter. It was reported that at this intermediate gelation level, a domain morphology was preserved, in which the interfaces between dense primary cores were not completely compacted. The presence of voids then led to a more extensive deformation and energy absorption during crack propagation.[47]

Besides this morphological effect, there are also different mechanisms because of the presence of nanofillers that can influence the overall fracture toughness, including filler/matrix debonding and void formation, shear yielding/banding, crazing, crack deflection, and crack pinning.[65–67]

Here, the dispersion and especially the nature of the interfacial layer plays a major role. In fact, cracks encounter rigid particles as obstacles, which can deviate and branch the crack front or even pin it, depending on the strength of the interface. A weak interface could represent a preferential path for the crack growth and, thus, compromise the resulting toughness,[68,69] and a too-strong one simply does not affect the crack propagation. When, on the contrary, the interface yields before the matrix, more extensive deformation can occur and, thus, increase the energy required for the crack to grow.[70,71] This was expected to occur with PAA- and PBAA-modified particles.

## CONCLUSIONS

In this article, results of PVC-based materials containing neat and differently modified calcium carbonate nanoparticles were discussed.

In particular, the surface of $CaCO_3$ was coated with PAA or PBAA, and for comparison, neat and commercial stearic acid modified nanoparticles were tested as fillers.

The gelation time of PVC was shortened as a function of filler addition because of a frictional heat developed as a consequence of good contact between the primary PVC particles and filler during the processing. A most pronounced decrease was recorded in the case of materials containing stearic acid modified nanoparticles (system A) as a result of a lubricant effect of the modifier.

DSC analysis underlined the permanence of residual primary particles, whose percentage was more than twice that in neat PVC in all of the samples containing modified $CaCO_3$. Morphological analysis proved the effectiveness of PAA and PBAA as coupling agents. In fact, both these materials (C–D) exhibited a typical nanostructured morphology in which nanoparticles were homogeneous and finely dispersed in the matrix. Moreover, the absence of pullout phenomena was clear evidence of good nanoparticle/PVC interfacial adhesion. Conversely, the addition of neat $CaCO_3$ generated serious debonding and agglomeration phenomena as a result of polymer/filler incompatibility. Finally, in the case of stearic acid modified nanoparticles, the coating agent prevented the debonding phenomena, but at the same time, it was not able to prevent $CaCO_3$ clustering.

A significant improvement in the thermal stability of PVC was obtained with the addition of neat and stearic acid modified nanoparticles. This finding could be ascribed to the ability of surface $Ca^{2+}$ ions to scavenge part of the HCl produced and reduce the extent of its autocatalytic effect in the dehydrochlorination process. The lower thermal stability of stearic acid with respect to PVC rendered available surface calcium ions before the dehydrochlorination process started and, thus, allowed the improvement of the thermal stability. Finally, the mechanical properties were evaluated at low and high deformation rates. The flexural modulus improved in the case of systems containing PAA- and PBAA-modified $CaCO_3$ as a result of the observed morphology. Also, the flexural strength increased for these systems; this confirmed good interactions occurring between the phases and the effectiveness of the surface modifiers as coupling agents.

With regard to the toughness, the permanence of residual primary particles in the systems was mainly responsible for an increase in $K_C$. The most pronounced improvement of $K_C$ in the case of C and D was considered a result of the morphology and elastic properties of the surface modifiers.

## References

1. Titow, W. V. PVC Technology, 4th ed.; Elsevier: New York, 1984.
2. Eastwood, E. A.; Dadmun, M. D. Polymer 2002, 43, 6707.
3. Chen, C. H.; Wesson, R. D.; Collier, J. R.; Lo, Y. W. J Appl Polym Sci 1995, 58, 1087.

4. Klaric, N.; Stipanelow, V.; Roje, U. J Appl Polym Sci 2000, 78, 166.
5. Robinovic, I. S. J Vinyl Addit Techonol 1983, 5, 179.
6. Yang, W. J.; Wu, Q. Y.; Zhou, L. L.; Wang, S. Y. J Appl Polym Sci 1997, 66, 1455.
7. Ratnam, T.; Zaman, K. Polym Degrad Stab 1999, 65, 99.
8. Dubois, P.; Alexandre, M. Adv Eng Mater 2006, 8, 147.
9. Jordan, J.; Jacob, K. I.; Tannenbaum, R. M.; Sharaf, A.; Jasiuk, I. Mater Sci Eng A 2005, 393, 1.
10. Raya; S.; Easteala, A. J. Mater Manuf Processes 2007, 22, 741.
11. Avella, M.; Errico, M. E.; Martelli, S.; Martuscelli, E. Appl Organomet Chem 2001, 15, 435.
12. Avella, M.; Cosco, S.; Di Lorenzo, M. L.; Di Pace, E.; Errico, M. E. J Therm Anal Calorim 2005, 80, 131.
13. Avella, M.; Errico, M. E.; Martuscelli, E. Nano Lett 2001, 1, 213.
14. Drzal, L. T.; Rich, M. J.; Koenig, M. F.; Lloyd, P. F. J Adhes 1983, 16, 133.
15. Berriot, J.; Montes, H.; Lequeux, F.; Long, D.; Sotta, P. Macromolecules 2002, 35, 9756.
16. Ramanathan, T.; Liu, H.; Brinson, L. C. J Polym Sci Part B: Polym Phys 2005, 43, 2269.
17. Ciprari, D.; Jacop, K.; Tannenbaum, R. Macromolecules 2006, 39, 6565.
18. Pukánszky, B. New Polym Mater 1992, 3, 205.
19. Jancar, J.; Kucera, J. Polym Eng Sci 1990, 30, 707.
20. Jancar, J.; Kucera, J. Polym Eng Sci 1990, 30, 714.
21. Sumita, M.; Tsukumo, Y.; Miyasaka, K.; Ishikawa, K. J Mater Sci 1983, 18, 1758.
22. Fekete, E.; Molnar, S. Z.; Kim, G. M.; Micher, G. H.; Pukanszky, B. J Macromol Sci Phys 1999, 38, 885.
23. Liang, Z. M.; Wan, C. Y.; Zhang, Y.; Wei, P.; Yin, J. J Appl Polym Sci 2004, 92, 567.
24. Ren, J.; Huang, Y. X.; Liu, Y.; Tang, X. Z. Polym Test 2005, 24, 316.
25. Wan, C. Y.; Zhang, Y.; Zhang, Y. X.; Qiao, X. Y.; Teng, G. M. J Polym Sci Part B: Polym Phys 2004, 42, 286.
26. Huang, Z.; Lin, Z.; Cai, Z.; Mai, K. Plast Rubber Compos Process Appl 2004, 33, 343.
27. Zhang, Q.; Yang, H.; Fu, Q. Polymer 2004, 45, 1913.
28. Zhang, J. Z.; Wang, X.; Lu, L. D.; Li, D.; Yang, X. J. J Appl Polym Sci 2003, 87, 381.
29. He, Y. J Powder Technol 2004, 59, 147.
30. Wu, D. Z.; Wang, X. D.; Song, Y. Z.; Jin, R. G. J Appl Polym Sci 2004, 92, 2714.
31. Zeng, X. F.; Chen, J. F.; Wang, G. Q. Acta Polym Symp 2002, 6, 738.
32. Sun, S.; Li, C.; Zhang, L.; Du, H. L.; Burnell-Gray, J. S. Polym Int 2006, 55, 158.
33. Chen, C.; Teng, C. C.; Su, S. F.; Wu, W. C.; Yang, C. H. J Polym Sci Part B: Polym Phys 2006, 44, 451.
34. Chen, N.; Wan, C. Y.; Zhang, Y.; Zhang, Y. X. Polym Test 2004, 23, 169.
35. Chen, N.; Wan, C. Y.; Zhang, Y.; Zhang, Y. X.; Zhang, C. J Appl Polym Sci 2005, 95, 953.
36. Xiong, Y.; Chen, G.; Guo, S. J Appl Polym Sci 2006, 102, 1084.
37. Yang, L.; Hu, Y.; Guo, H.; Song, L.; Chen, Z.; Fan, W. J Appl Polym Sci 2006, 102, 2560.
38. Bakar, A. A.; Mohmed Rosli, N. N. J Tekn 2006, 45, 83.
39. Utracki, L. A. Polymer Blends Handbook; Springer-Verlag: New York, 2002.
40. Metz, G.; Wu, X.; Smith, S. O. J Magn Reson Ser A 1994, 110, 219.
41. Cook, R. L.; Langford, C. H.; Yamadagni, R.; Preston, C. M. Anal Chem 1996, 68, 3979.
42. Wunderlich, B. Thermal Analysis; Academic: Boston, 1909.
43. ASTM D 256-06ae1, Standard Test Methods for Determining the Izod Pendulum Impact Resistance of Plastics; American Society for Testing and Materials: West Conshohocken, PA, 1993.
44. ASTM D 790-07e1, Standard Test Methods for Flexural Properties of Unreinforced and Reinforced Plastics and Electrical Insulating Materials; American Society for Testing and Materials: West Conshohocken, PA, 2007.
45. Drzal, L. T.; Rich, M. J.; Koenig, M. F.; Lloyd, P. F. J Adhes 1983, 16, 133.
46. Wah, C. A.; Choong, L. Y.; Neon, G. S. Eur Polym J 2000, 36, 789.
47. Alves, J. P. D.; Rodolfo, A.,Jr. Polímeros 2006, 16, 165.
48. Teh, J. W.; Cooper, A. A.; Rudin, A.; Batiste, J. H. L. J Vinyl Addit Technol 1989, 11, 33.
49. Fillot, L.-A.; Hajji, P.; Gauthier, C.; Masenelli Verlot, K. J Vinyl Addit Technol 2006, 12, 98.
50. Covas, J. A.; Gilbert, M. Polym Eng Sci 1992, 32, 743.
51. Endo, K.; Saitoh, M. Macromol Rapid Commun 2002, 23, 913.
52. Krzewki, R. J.; Collins, E. A. J Macromol Sci Phys 1981, 20, 465.
53. Cornwell, D. W. Ind Miner 2001, July, 35.
54. Comeaux, E. J.; Chen, C. H.; Collier, J. R.; Wesson, R. D. Polym Bull 1994, 33, 701.
55. Chen, C.-H.; Mao, C.-F.; Lo, Y.-W. J Appl Polym Sci 2001, 81, 3022.
56. Gilbert, M.; Vyvoda, J. C. Polymer 1981, 219, 1134.
57. Potente, H.; Schultheis, M. S. Kunststoffe 1987, 77, 401.
58. Kuriyama, T.; Narisawa, I.; Shina, R.; Kotaki, M. J Vinyl Addit Technol 1998, 4, 164.
59. Starnes, W. H. Prog Polym Sci 2002, 27, 2133.
60. Karayildirim, T.; Hsu, C.-K.; Lee, J.-S. J Anal Appl Pyrolysis 2006, 75, 112.
61. Jaw, K.-S.; et al. Thermochim Acta2001,367–368,165.
62. Sell, T.; Vyazovkin, S.; Wight, C. A. Comb Flame 1999, 119, 174.
63. Don, T. M.; Chuang, C.-Y.; Chiu, W.-Y. Tamkang J Sci Eng 2002, 5, 235.
64. Dányádi, L.; Renner, K.; Móczó, J.; Pukánszky, B. Polym Eng Sci 2007, 47, 1246.
65. Argon, A. S.; Cohen R. E. Polymer 2003, 44, 6013.
66. Kim, G.-M.; Michler, G. H. Polymer 1998, 39, 5689.
67. Cotterell, B.; Chia, J. Y. H.; Hbaieb, K. Eng Fract Mech 2007, 74, 1054.
68. Yuan, Q.; Misra, R. D. K. Polymer 2006, 47, 4421.
69. Chen, G.; Tian, M.; Guo, S. J Macromol Sci Phys 2006, 45, 709.
70. Qiang, F.; Guiheng, W.; Chunxiao, L. Polymer 1995, 36, 2397.
71. Zeng, X.; Wang, W.; Wang, G.; Chen, J. J Mater Sci 2008, 43, 3505.